JOURNAL OF THERMOPHYSICS AND HEAT TRANSFER
Vol. 20, No. 3, July–September 2006

Technical Notes

TECHNICAL NOTES are short manuscripts describing new developments or important results of a preliminary nature. These Notes should not exceed 2500 words (where a figure or table counts as 200 words). Following informal review by the Editors, they may be published within a few months of the date of receipt. Style requirements are the same as for regular contributions (see inside back cover).

Synthesis and Characterization of $Zn_{1-x}Mg_xO$ Thin Films

P. Raji* and K. Ramachandran†
Madurai Kamaraj University,
Madurai 625 021, Tamilnadu, India
and
C. Sanjeeviraja‡
Alagappa University, Karaikudi 630 003, Tamilnadu, India

Nomenclature

C_p = specific heat
D = thermal diffusivity
E = incident photon energy
l = thickness of sample
α = absorbance
λ = thermal conductivity
ρ = density

I. Introduction

In the past several years, a great deal of research effort on wide-band gap semiconductors has resulted in the commercialization of group 3 nitride-based blue lasers, light emitting diodes, optical data storage, and solar cell applications.[1] As an alternative to GaN (the group 3 nitride), ZnO has now come into existence due to the large binding energy (~60 meV) that results in extremely efficient emission with room-temperature optically pumped lasing when ZnO is in the form of thin films and microcrystallites[2] are made available.

To explore a material with a shorter UV emission, one of the techniques is to dope other ions into the lattice.[1] To obtain high-performance light-emitting diodes, the key technique is to construct a heterojunction to realize double confinement for electrons and photons in optoelectronic devices. The closeness of the lattice parameters of MgO and ZnO makes it possible to modulate the bandgap in $Zn_{1-x}Mg_xO$ thin films.[3] Also, the ionic radius of Mg^{2+} (0.57 Å) is similar to that of Zn^{2+} (0.60 Å); thus, a wide range of solubility for Mg in the zinc blend is easily possible in the film.

Alloying ZnO films with MgO or CdO potentially permits the bandgap to be controlled between 3.4 and 4 eV and higher. This also suggests the possibility of hybrid optoelectronic devices comprised of lattice matched MgZnO/AlGaN heterojunctions.[4] Recently, Murakawa et al.[5] showed that MgZnO film on an Si substrate has many applications in optoelectronic technology.

Among the numerous physical properties of semiconducting materials, the thermal properties are the most important for improvement of the performance of any thermocontrolled and energy devices.

Similarly, the MgZnO/ZnO heterostructure for optoelectronics devices requires precise knowledge of the fundamental optical properties of ZnO and its alloys.

Here, we report our measurements of the thermal properties of polycrystalline $Zn_{1-x}Mg_xO$ thin film synthesized on a glass substrate by electron beam evaporation by using photoacoustics because this method can measure the thermal conductivity without making physical contact on the sample.[6]

II. Experiment

$Zn_{1-x}Mg_xO$ thin films were prepared by electron beam evaporation using a HINDHIVAC vacuum coating unit (Model 12A4D) with an electron beam power supply (Model EBG-PS-3K). The $Zn_{1-x}Mg_xO$ target was sintered at 300°C after grinding the polycrystalline MgO and ZnO powder (each with a purity of 99.9%) in a furnace. The powder was made into pellets, and these were then placed in graphite crucibles on the water-cooled copper hearth of the electron gun inside the vacuum chamber. In the electron gun, the electrons were extracted from a dc heated tungsten filament cathode, through the electric field, past the anode, and deflected through an angle ~180°C by the magnetic field to reach the target material. The surface of the $Zn_{1-x}Mg_xO$ pellets on the graphite crucible was scanned by the resultant and deflected electron beam with an accelerating voltage of 5 kV and a power density of ~1.5 $kW \cdot cm^{-2}$. The ablated material evaporated, and the evaporated vapor phase condensed and deposited as thin films on the glass substrates. During the deposition process, the chamber was evacuated in a high vacuum of order 1×10^{-5} mbar using rotary and diffusion pumps. The homogeneous distribution of evaporation of $Zn_{1-x}Mg_xO$ particles on the substrate surface was achieved by the continuous rotation of the substrate, positioned 20 cm above the target material. The depositions were carried out at room temperature. Such films were synthesized for different Mg concentrations ($x = 0.1$, 0.2, and 0.3).

III. Structural Properties

The crystalline structure of the grown films is characterized by x-ray diffraction (XRD) (Philips X' pert System, CuK_α 1.5418 Å). The XRD patterns of the two samples ZnO and $Zn_{0.9}Mn_{0.1}O$ are presented in Fig. 1. There are three main peaks in the spectra, which belong to the (100), (002), and (101) planes of the ZnO wurzite structure.

No peak originating from other compounds is detected, except those of ZnO. The ZnO film exhibits a preferential orientation of a (002) plane.

Compared with ZnO thin films, the diffraction angle of the (002) plane is larger in the $Zn_{1-x}Mg_xO$ films. This indicates that the Zn^{2+} ions are successfully substituted by Mg^{2+} ions in the ZnO lattice.

Also, note that all of these films are oriented in the c axis and become weak when the Mg content in the films increases.

IV. Optical Properties

The optical transmittance is measured for all of the samples by using an UV–visible spectrophotometer (Perkin Elmer lambda). Figure 2 shows transmittance spectra of ZnO and $Zn_{0.8}Mg_{0.2}O$ only. Compared to ZnO film, in $Zn_{0.8}Mg_{0.2}O$, the absorption edge shifts from 380 to 340 nm. Such measurements for the other films are also carried out, and the shift is from 380 to 320 nm for $x = 0$ to 0.3.

Received 10 November 2005; revision received 21 November 2005; accepted for publication 22 November 2005.

*Research Scholar, School of Physics; rajimku@rediffmail.com.
†Professor, School of Physics; thirumalchandran@yahoo.com.
‡Professor, Department of Physics; sanjeeviraja@rediffmail.com.

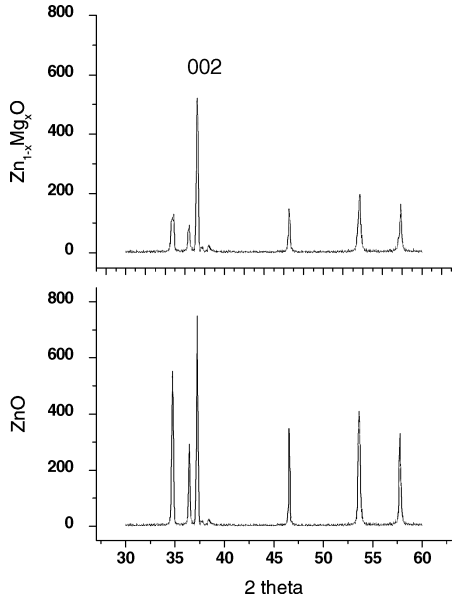

Fig. 1 XRD pattern of ZnO and $Zn_{0.9}Mg_{0.1}O$.

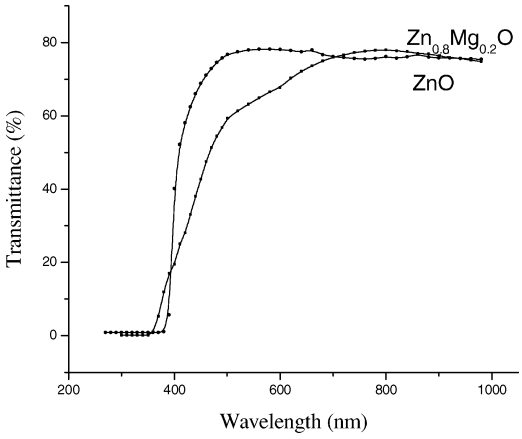

Fig. 2 UV–visible spectrum of ZnO and $Zn_{0.8}Mg_{0.2}O$.

Based on the UV–visible transmittance measurements, the bandgap of the $Zn_{1-x}Mg_xO$ films was obtained by plotting α^2E^2 vs E. The bandgap increases from 3.27 to 3.8 eV for $x = 0$–0.3, which is an indication of $Zn_{1-x}Mg_xO$ alloys by the Mg incorporation.

As the Mg content increases, the absorption edge moves toward the higher energy side. This indicates that the introduction of Mg increases the bandgap of ZnO by pushing the conduction band edge upward.

V. Photo Acoustics (PA)

When a modulated light is absorbed by the sample located in a sealed cell, the nonradiative decay of the absorbed light produces a modulated transfer of heat to the surface of the sample, which produces pressure waves in the gas inside the cell that can be detected by the microphone attached to the cell.[7] The present photoacoustic spectrometer has a 400-W Xe lamp (Jobin Yvon) beam intensity is mechanically chopped by an electromechanical chopper (Model PAR 650) and focused onto the sample through a monochromator (Model Triax 180, Jobin Yvon). The sample is placed in the photoacoustic (PA) cell and the microphone is placed very near the sample. The PA cell is a nonresonant type and is made of stainless steel. The PA signal from the microphone is fed to a lock-in amplifier (Model Perkin Elmer 7225 DSP). The setup is shown in Fig. 3.

VI. PA Measurements

Because, whatever PA measurements are made on thin films would give only the effective value of glass substrate and the

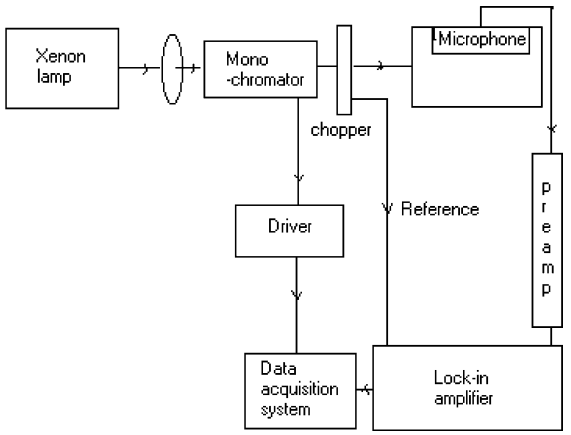

Fig. 3 PA spectrometer.

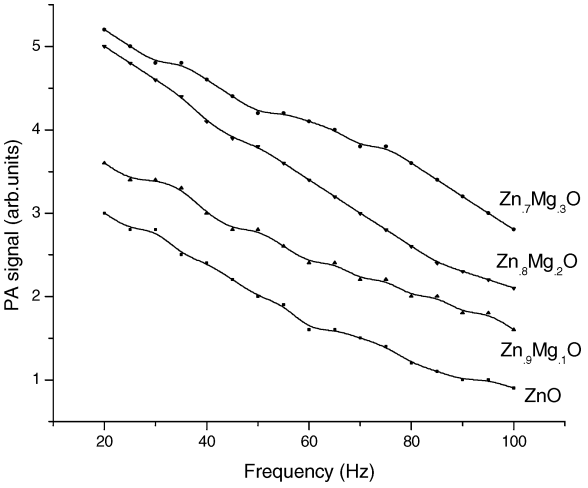

Fig. 4 Depth profile for ZnO and $Zn_{1-x}Mg_xO$.

$Zn_{1-x}Mg_xO$ film, proper deconvolution is necessary to deduce the value of the film. This is basically done by a two-layer model.

The effective thermal diffusivity of the two layer system can be written as[8]

$$D = 1 \Big/ \left[\frac{x^2}{D_1} + \frac{(1-x)^2}{D_2} + x(1-x)\left(\frac{\lambda}{D_1} + \frac{1}{\lambda D_2} \right) \right] \quad (1)$$

where $x = l_1/l$ is the fraction of thickness of material 1 in the composite system (glass and film) and $\lambda = \kappa_1/\kappa_2$.

Similarly, the effective thermal conductivity is given as

$$l/\kappa = (l_1/\kappa_1) + (l_2/\kappa_2) \quad (2)$$

where κ_1 and κ_2 are thermal conductivities of glass and the film, respectively.

A. Depth Profile Analysis

The depth profile analysis by PA is carried out for two cases: 1) glass plate deposited with the film and 2) glass plate alone, that is, first the glass plate with the thin film coat is taken inside the PA cell and then the PA signal is observed for different chopping frequencies. This is shown in Fig. 4.

If f_c is the characteristic frequency of the sample of thickness l, then the thermal diffusivity can be calculated from

$$D = f_c l^2 \ \mathrm{m^2 s^{-1}} \quad (3)$$

The thermal conductivity is

$$\kappa = D\rho C_p \mathrm{W m^{-1} \cdot K^{-1}} \quad (4)$$

where C_p is the specific heat capacity of the sample. The density and specific heat are calculated from Vegard's law for the bulk ZnO

Table 1 Thermal properties of $Zn_{1-x}Mg_xO$ films

Sample	Thermal diffusivity, $m^2/sec \times 10^{-6}$	Thermal conductivity, $W/m \cdot K$	Thermal conductivity, $W/m \cdot K$ (bulk)[9]
ZnO	2.31	6.72	7.1
$Zn_{0.9}Mg_{0.1}O$	3.54	7.43	——
$Zn_{0.8}Mg_{0.2}O$	4.76	8.95	——
$Zn_{0.7}Mg_{0.3}O$	5.89	10.12	——

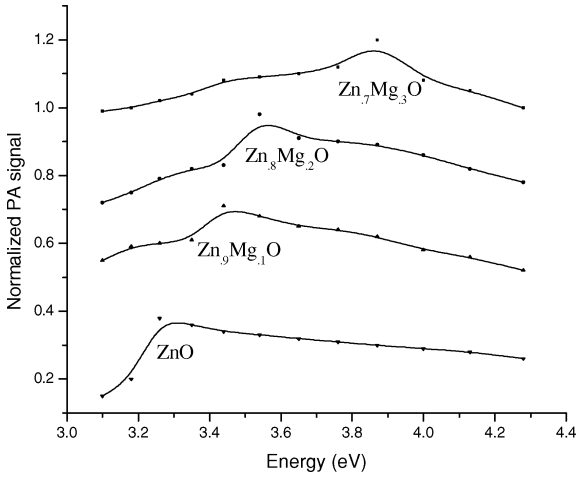

Fig. 5 PA spectrum of ZnO and $Zn_{1-x}Mg_xO$.

and MgO, and, as a first approximation, this value is used for the thin film.

Such measurements are performed for the other $Zn_{1-x}Mg_xO$ thin films also. Now, with the glass plate alone as the sample, the PA measurements were performed as usual and, with these two sets of data on thermal diffusivity of the glass plate and the effective thermal diffusivity of glass plate and the film, thermal diffusivity for the film alone is computed from Eq. (1). Such diffusivities of the various $Zn_{1-x}Mg_xO$ thin films thus measured are given in Table 1.

B. PA Spectrum

The PA power detected will be proportional to the absorption of the optical energy by the sample. The PA spectrum for $Zn_{1-x}Mg_xO$ was obtained by recording the PA signal as a function of the wavelength of the incident beam for a constant modulation frequency. The PA spectrum for each sample is normalized using the PA spectrum obtained for carbon black. From the PA amplitude-wavelength plot, the energy gap is determined corresponding to the preliminary peak, and calculated using the relation, and it is given in Fig. 5, as the present system has a direct band gap.

VII. Results and Discussions

We reported the thermal diffusivity and bandgap of $Zn_{1-x}Mg_xO$ film by PA spectroscopy. The thermal diffusivity of ZnO film is less than the bulk ZnO, and the thermal diffusivity of this film increases with the increasing concentration of Mg.

There are many experimental reports available to justify the reduction (up to 50%) in thermal conductivity in semiconductor thin films compared to bulk.[10–12] This is basically due to the phonon mean free path, that is, when the film thickness is of the order of the phonon mean free path scattering is bound to occur that would reduce the thermal conductivity. Even though there are other possible reasons for the reduction of its thermophysical properties such as 1) doping effect, 2) interface scattering of phonons, and 3) quantum size effects, the doping effect is not a major factor.

The quantum size effects will be important when the phonon mean free path is larger than the thickness of the individual layer. This suggests that the observed large reduction mainly stems from the interface scattering effects. Thus, the reduction in thermal diffusivity, and, hence, the thermal conductivity of ZnO film, is essentially due to increased collisions.

In the present work, it is observed that the thermal diffusivity of ZnO film increases with the concentration of Mg added. This type of behavior has already been reported.

Firszt et al.[13] have studied the optoelectronic and thermal properties of ZnSe, $Zn_{0.7}Mg_{0.3}Se$, and $Zn_{0.88}Be_{0.12}Se$ crystals. Compared with thermal diffusivity of ZnSe, the admixture of Be, Mg, or Mn elements causes a small increase in thermal diffusivity.

Similarly, the bandgaps of the $Zn_{1-x}Mg_xO$ thin films are measured by PA, and increase from 3.3 to 3.8 eV as the concentration increases from $x = 0$ to 0.3.

Recently, Zhang et al.[14] have studied the $Zn_{1-x}Mg_xO$ thin films grown by an ultrasonic spray pyrolysis method. The photoluminescence spectra exhibit one peak located in the UV region that originates from the excitonic near the bandgap emission. The bandgaps increase from 3.26 to 3.54 eV from $x = 0$ to 0.2. Our measurements on bandgap by PA also lie in the range from 3.3 to 3.8 eV.

Thus, $Zn_{1-x}Mg_xO$ films can be considered not only as barrier layers for the ZnO active layer, but also as UV light-emitting material, the luminescence energy of which can be tuned from 3.3 ($x = 0$) to 3.8 eV ($x = 0.30$) by adjusting the Mg content x.

VIII. Conclusions

$Zn_{1-x}Mg_xO$ thin films were obtained by an electron beam evaporation method. The optical bandgap is found to vary from 3.4 to 3.8 eV by adjusting the Mg content as seen from PA, and UV–visible. The advantage of this present method is that it is a contactless (with the sample) method, and so the results will be more reliable.

Thermal conductivity increases with the concentration of Mg in thin films, and these values are given here by a PA method. It is well accepted that the four-probe method is the conventional technique for such measurements. However, PA is also a reliable tool for the same measurements because one can directly measure the thermal diffusivity without making contact with the sample.

Thermal diffusivity and, hence, the thermal conductivity of ZnO films increase as the concentration of Mg doping is increased. This again can be visualized through phonons.

When ZnO is doped with Mg, localized vibrational modes appear as the mass defect parameter, $\varepsilon = 1 -$ (mass of Mg/mass of Zn) (0.63), which is very appreciable. These additional phonons appear outside the cutoff frequency of the host ZnO system. This additional but not generally allowed phonon in the host system contributes to the thermal diffusion. Thus, on doping of a thin film with such a mass defect, we expect an increased value for thermal diffusivity or thermal conductivity.

References

[1]Pcarton, S. J., Zolper, J. C., Shul, R. J., and Ren, F., "GaN: Processing, Defects and Devices," *Journal of Applied Physics*, Vol. 86, No. 1, 1999, pp. 1–78.

[2]Reynolds, D. C., Look, D. C., and Jogai, B., "Optically Pumped Ultraviolet Lasing from ZnO," *Solid State Communications*, Vol. 99, No. 12, 1996, pp. 873–875.

[3]Hayashi, I., Panish, M. B., Foy, P. W., and Sumski, S., "Junction Lasers Which Operate Continuously at Room Temperature," *Applied Physics Letters*, Vol. 17, No. 3, 1970, pp. 109–111.

[4]Vispute, R. D., Talyansky, V., Choopun, S., Sharma, R. B., Venkatesan, T., Tang, M. Hc. X., Halpern, J. B., Speneer, M. G., Li, Y. X., Salamanca Riba, L. G., Iliadis, A. A., and Jones, K. A., "Heteroepitaxy of ZnO and GaN and Its Implications for Fabrication of Hybrid Optoelctronic Devices," *Applied Physics Letters*, Vol. 73 , No. 3, 1998, pp. 348–350.

[5]Murakawa, T., Fukudome, T., Hayashi, T., Isshiki, H., and Kimura, T., "Structural and Optical Properties of $Mg_xZn_{1-x}O$ Thin Films Formed by Sol–Gel Method," *Physica Status Solidi (c)*, Vol. 1, No. 10, 2004, pp. 2564–2568.

[6]Bataka, N. T., Kobayashi, T., Sekine, D., and Izumi, T., "Thermal Characterization of CVD Diamond Film by Photoacoustic Method," *Appl.Surface.Sci.*, Vol. 159–160, 2000, pp. 594–598.

[7]Rosencwaig, A., and Gersho, A., "Theroy of Photoacoustic Effect with Solids," *Journal of Applied Physics*, Vol. 47, No. 1, 1976, pp. 64–69.

[8]Alvarado-Gil, J. J., Zelaya-Angel, O., and Sanchez-Sinencio, F., "Photoacoustic Thermal Characterization of a Semiconductor (CdTe)–Glass Two Layer System," *Vacuum*, Vol. 46, No. 8–10, 1995, pp. 883–886.

[9]Boggs, S., Kuang, J., Andoh, H., and Nishiwaki, S., *IEEE Transactions on Power Delivery*, Vol. 15, No. 2, 2000, pp. 562–568.

[10]Ju, Y. S., and Goodson, K. E., "Phonon Scateering in Silicon Films with Thickness of Order 100 nm," *Applied Physics Letters*, Vol. 74, No. 2, 1999, pp. 3005–3007.

[11]Chen, G., "Phonon Wave Heat Conduction in Thin Films and Superlattices," *Journal of Heat Transfer*, Vol. 121, 1999, pp. 945–953.

[12]Asheghi, M., Leung, Y. K., Wong, S. S., and Goodson. K. E., "Phonon Boundary Scattering in Thin Silicon Layers," *Applied Physics Letters*, Vol. 71, No. 13, 1997, pp. 1798–1800.

[13]Firszt, F., Legowski, S., Marasek, A., Meczynska, H., Pawlak, M., and Zakrzewski, J., "Photoelectric and Photothermal Properties of Selected II-VI Mixed Crystals," *Optoelectronics Review*, Vol. 12, No. 1, 2004, pp. 161–164.

[14]Zhang, X., Li, X. M., Chen, T. L., Zhang, C. Y., and Yu, W. D., "P Type Conduction in Wide Gap $Mg_xZn_{1-x}O$ Films Grown by Ultrasonic Spray Pyrolysis," *Applied Physics Letters*, Vol. 87, Aug. 2005, pp. 092101–092103.